involve

Visual representation of the Riemann and Ahlfors maps via
the Kerzman–Stein equation

Michael Bolt, Sarah Snoeyink and Ethan Van Andel

Visual representation of the Riemann and Ahlfors maps via the Kerzman–Stein equation

Michael Bolt, Sarah Snoeyink and Ethan Van Andel

(Communicated by Michael Dorff)

The Szegő kernel serves as one of the canonical functions associated to a region in the complex plane, and from it one can compute the Riemann (or Ahlfors) map, the essentially unique conformal transformation of the region to the unit disc. We provide an elementary description of the method that Kerzman and Stein used to compute the Szegő kernel, and subsequently, the Riemann and Ahlfors maps. A description, too, is provided for a new tool that generates visual representations of these functions and is included with the open-source computer algebra system Sage.

1. Introduction

In his Ph.D. thesis in 1851, Bernhard Riemann stated a theorem that has come to be regarded as one of the most important results in complex analysis. It says that no matter how pathological the boundary of a simply connected (open) region, one can map the region to the unit disc in such a way that angles are preserved.

Theorem 1 (Riemann mapping theorem). *Let Ω be a* (*nonempty*) *simply connected region in the complex plane that is not the entire plane. Then, for any $z_0 \in \Omega$, there exists a bianalytic map f from Ω to the unit disc such that $f(z_0) = 0$ and $f'(z_0) > 0$.*

To illustrate the result, Figure 1 shows a map for a triangular region, using colors and contour lines to identify the corresponding points of the transformation. (The colors are visible in the electronic version of this paper.) In this example the orthocenter is mapped to the origin without rotation at this point. We generated these images using a new tool, `Riemann_Map()`, that the third author developed to accompany Sage, a freely available, open-source computer algebra system. The tool is now included in the core Sage library, and using a web browser, one can generate similar pictures on any computer that has an internet connection.
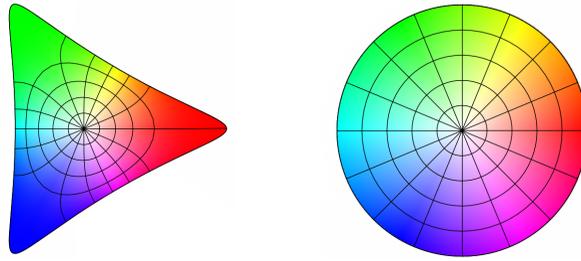
Figure 1. Left: color plot and overlay for the Riemann map of a triangular region. Right: the color scheme for the unit disc.

Although Riemann stated his result in 1851, the first rigorous proof came much later and is due to Carathéodory in 1912. Other proofs have appeared since then, but not all of them provide an easy way to compute the Riemann map. For a proof that is related to the methods used in this paper, see [Garabedian 1991].

The purpose of this paper is threefold. First, we provide a simple description of the method that Kerzman and Stein [1978] used to compute the Riemann map which is based on the Szegő kernel. Next, we provide adaptations of the theory in order to accommodate the case of a multiply connected region and to permit more accurate calculations near the corners of a simply connected region whose boundary is piecewise differentiable. Finally, we describe the numerical implementation of the method and the key features of the tool `Riemann_Map()`, including an adaptation for generating images of the Ahlfors map for a general multiply connected region.

Our implementation of the Nyström method for solving the Kerzman–Stein integral equation is like that used in [Kerzman and Trummer 1986]. Subsequently, that method was modified in [Trummer 1986; O'Donnell and Rokhlin 1989; Murid et al. 1998]. To visualize the Riemann map and Ahlfors map, we use a method devised by Frank Farris [1998] that he calls domain coloring and which uses a color's brightness and hue to indicate the value of a complex function. We mention
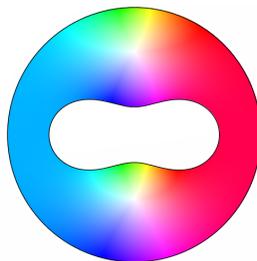
Figure 2. The Ahlfors map for a 2-connected region without a contour overlay. (Color scheme is the same as that of Figure 1.)

that `Riemann_Map()` accepts as data the boundary of a region, given either as a parametrized curve or as a set of boundary points to be interpolated. Using a personal machine, the tool can generate accurate pictures in just seconds.

For ease of presentation, we limit the discussion to regions whose boundary is infinitely differentiable. This means that the boundary curves have a curvature function that is infinitely differentiable with respect to the arc length parameter. The ideas are essentially the same for a twice differentiable region, and many of the results apply even in a still more general context. In particular, `Riemann_Map()` works for domains with piecewise smooth boundary. For a justification of this point, see [Thomas 1996].

The reader who wishes to know more about complex variables than is presented here is encouraged to refer to [Bell 1992; Boas 2010; D'Angelo 2010]. (Bell [1992] offers a completely rigorous treatment of complex analysis in the manner of Kerzman and Stein.) The reader, though, who already has a good grasp of the subject can skip to the last section for an abbreviated users manual for `Riemann_Map()`. We encourage other faculty and student researchers to consider disseminating their work via a platform like Sage. Indeed, we found the review process to be a supportive one, and we were able to get started with relatively little experience working with the programming language Python.

2. Analytic functions and the Cauchy integral formula

The Riemann map and Ahlfors map are examples of analytic functions. For a region $\Omega \subset \mathbb{C}$, there are three equivalent formulations for what this means.

The simplest formulation says that a function $f : \Omega \to \mathbb{C}$ is analytic provided that near any point $z_0 \in \Omega$, it can be expressed as the sum of a power series

$$f(z) = \sum_{j=0}^{\infty} a_j (z - z_0)^j.$$

In fact, when this is the case, the coefficients a_j are the Taylor coefficients for f and are related to the derivatives of f via $a_j = f^{(j)}(z_0)/j!$. The second formulation says that f is analytic provided its real and imaginary parts, $u = \operatorname{Re} f$ and $v = \operatorname{Im} f$, satisfy the partial differential equations,

$$\frac{\partial u}{\partial x} = \frac{\partial v}{\partial y} \quad \text{and} \quad \frac{\partial u}{\partial y} = -\frac{\partial v}{\partial x},$$

which are known as the Cauchy–Riemann equations. This formulation permits an easy demonstration that the real and imaginary parts of an analytic function are harmonic, that is,

$$\triangle u \stackrel{\text{def}}{=} u_{xx} + u_{yy} = 0 \quad \text{and} \quad \triangle v \stackrel{\text{def}}{=} v_{xx} + v_{yy} = 0.$$

The third formulation is familiar from calculus. In this case f is analytic if it is everywhere differentiable, that is,

$$f'(z_0) \overset{\text{def}}{=} \lim_{h \to 0} \frac{f(z_0 + h) - f(z_0)}{h}$$

exists at each $z_0 \in \Omega$, where it is important to note that h is assumed complex. Of course it is easy to see from this formulation that polynomials with variable z are analytic—one proceeds in the same way as one would compute f' in calculus. We leave for the reader the additional exercise that $f(z) = |z|^2 = z\overline{z}$ is *not* analytic according to this formulation.

Essential to the Kerzman and Stein method is the Cauchy integral formula, one of the most basic results in complex analysis. It says that an analytic function can be expressed as an average of its values along a bounding curve.

Theorem 2 (Cauchy integral formula). *Let f be analytic in a simply connected region $\Omega \subset \mathbb{C}$ and let γ be a simple closed positively oriented curve in Ω. If z_0 is a point that lies interior to γ, then*

$$f(z_0) = \frac{1}{2\pi i} \int_{w \in \gamma} \frac{f(w)\, dw}{w - z_0}.$$

We mention that the equivalence of the second and third formulations of analyticity requires only a small amount of multivariable calculus. To see that a function which is analytic by the first formulation is analytic by the third formulation, one differentiates term-by-term using the standard results about power series. To see that a function which is analytic by the second formulation is analytic by the first formulation, one uses the Cauchy integral formula. The argument needed for this will be apparent after reading the next section.

3. The Cauchy projector

The Kerzman and Stein method begins with the observation that for a general function f defined on the boundary of a region, the Cauchy integral defines an analytic function $\mathscr{C}f$ inside the region. In particular, if one defines

$$\mathscr{C}f(z) = \frac{1}{2\pi i} \int_{w \in \partial\Omega} \frac{f(w)\, dw}{w - z} \quad \text{for } z \in \Omega,$$

then $\mathscr{C}f$ is analytic inside Ω. To see this, one expands $(w - z)^{-1}$ in a small disc centered at any $z_0 \in \Omega$ using the geometric series,

$$\frac{1}{w - z} = \frac{1}{w - z_0}\left[1 + \frac{z - z_0}{w - z_0} + \left(\frac{z - z_0}{w - z_0}\right)^2 + \left(\frac{z - z_0}{w - z_0}\right)^3 + \cdots\right].$$

The coefficients of the power series for $\mathscr{C}f$, centered at z_0, are then obtained by integration,

$$a_j = \frac{1}{2\pi i} \int_{w \in \partial\Omega} \frac{f(w)\, dw}{(w - z_0)^{j+1}}.$$

For a function f that is integrable on $\partial\Omega$, the series is sure to converge in any disc small enough to fit inside Ω, i.e., small enough for the geometric series to converge for every $w \in \partial\Omega$.

It follows, too, from the Cauchy integral formula, that if f begins as the boundary values of a function that is analytic inside Ω, then the Cauchy integral reproduces the values of that analytic function.

By finally calling on some approximation theory, we are then able to identify a context in which the Cauchy integral behaves as a projection operator. The theory shows that if f begins as an infinitely differentiable function on the boundary, then the function $\mathscr{C}f$, at first defined inside the region, extends continuously and infinitely differentiably on the closure of the region. For the proof of this fact we refer to the first chapter of [Bell 1992].

To help summarize our observations, let $C^\infty(\partial\Omega)$ denote the space of functions that are infinitely differentiable on the boundary and let $A^\infty(\partial\Omega)$ denote the subspace of functions that extend continuously and analytically inside the region. These are vector spaces over $\mathbb{C}$ and $A^\infty(\partial\Omega)$ is a subspace of $C^\infty(\partial\Omega)$. We have then established that the Cauchy integral maps $C^\infty(\partial\Omega)$ to $A^\infty(\partial\Omega)$, and it acts identically on $A^\infty(\partial\Omega)$. Although one might argue that there is an abuse of notation, we will write $\mathscr{C} : C^\infty(\partial\Omega) \to A^\infty(\partial\Omega)$ for this projection operator.

To illustrate the construction, we give a direct calculation for the unit disc. We begin with a general function f, defined on the unit circle, that can be expressed as a Fourier series

$$f(e^{it}) = \sum_{j=-\infty}^{\infty} a_j e^{ijt} = \sum_{j \geq 0} a_j e^{ijt} + \sum_{j < 0} a_j e^{ijt}.$$

Using the boundary parametrization, $w(t) = e^{it}$ for $0 \leq t < 2\pi$, and expressing in polar form, $z = re^{is}$ for $0 \leq r < 1$ and $0 \leq s < 2\pi$, we evaluate the Cauchy integral by expanding the kernel in a geometric series,

$$\mathscr{C}f(re^{is}) = \frac{1}{2\pi i} \int_0^{2\pi} \frac{f(e^{it})\, i e^{it}\, dt}{e^{it} - re^{is}} = \frac{1}{2\pi} \int_0^{2\pi} \sum_{k=0}^{\infty} r^k e^{ik(s-t)} \sum_{j=-\infty}^{\infty} a_j e^{ijt}\, dt$$

$$= \sum_{j \geq 0} a_j r^j e^{ijs}.$$

(The last step uses the fact that $\int_0^{2\pi} e^{int}\, dt = 2\pi$ if $n = 0$; the integral is zero

otherwise.) We conclude that $\mathscr{C}f(z) = \sum_{j \geq 0} a_j z^j$. Then letting $r \uparrow 1$ gives

$$\mathscr{C}f(e^{it}) = \sum_{j \geq 0} a_j e^{ijt}.$$

For reference, we mention that the situation should be reminiscent of linear algebra, where projection operators map finite dimensional spaces onto lower dimensional subspaces. To illustrate, identify points with position vectors and consider the operator that is represented using the standard basis by the matrix $\left(\begin{smallmatrix} 0 & 2 \\ 0 & 1 \end{smallmatrix}\right)$. This operator maps points in $\mathbb{R}^2$ to points on the line $x - 2y = 0$, and it does so in such a way that points on the line are preserved. We leave these easy facts for the reader to check, and we return to the example in the next section.

Like the example from linear algebra, we mention that the Cauchy projector is linear, since integration is a linear process. In particular, $\mathscr{C}(f + \lambda g) = \mathscr{C}f + \lambda \mathscr{C}g$ for $\lambda \in \mathbb{C}$. A fundamental difference, though, is the fact that the Cauchy projector acts between infinite dimensional spaces, as is evident in the example of the unit disc. As will be seen in the next section, however, its skew-hermitian part behaves like its finite dimensional counterpart.

4. The Szegő projector and the Kerzman–Stein equation

We saw in Section 3 that the Cauchy integral provides a projection from $C^\infty(\partial\Omega)$ to $A^\infty(\partial\Omega)$. But the projection is not generally *orthogonal*. To illustrate, Figure 3 shows two projections from $\mathbb{R}^2$ onto the line $x - 2y = 0$. The first is the projection described at the end of the last section, and the second is the orthogonal (shortest distance) projection of $\mathbb{R}^2$ onto the same line.

To make sense of this one needs a notion of distance. In the linear algebra example, distance is measured in the Euclidean way, and this distance arises from the standard dot product. The analogous inner product for functions is given by

$$(f, g) = \int_{\partial\Omega} f\overline{g}\,ds,$$

where ds indicates that integration is done with respect to arc length. The norm of a function is then given by $\|f\| = \sqrt{(f, f)}$ and the distance between functions
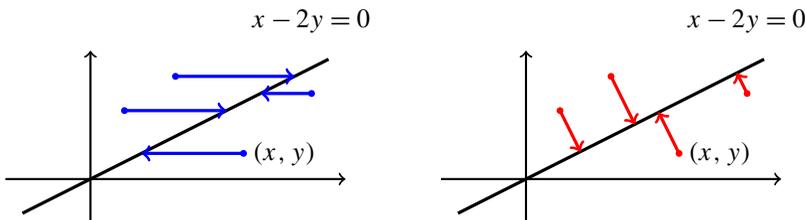
Figure 3. Nonorthogonal and orthogonal projections to $x - 2y = 0$.

is the norm of their difference. Finally, the Szegő projector can be defined as the *orthogonal* projection,

$$\mathscr{S} : C^\infty(\partial\Omega) \overset{\perp}{\to} A^\infty(\partial\Omega).$$

At first it may not be obvious that $A^\infty(\partial\Omega) \subset C^\infty(\partial\Omega)$ is a *closed* subspace — a nontrivial fact since both spaces are infinite dimensional. In particular, it may not be obvious that the Szegő projector maps an infinitely differentiable function to an infinitely differentiable function. These properties, however, can be shown to follow as consequences of the Kerzman and Stein theory. We again refer to [Bell 1992] for a treatment of these delicate facts.

The key insight behind the Kerzman and Stein theory can be described now as follows. The Cauchy integral provides an explicitly computable, though generally nonorthogonal, projection $\mathscr{C} : C^\infty(\partial\Omega) \to A^\infty(\partial\Omega)$. Meanwhile, the Szegő projector represents the uniquely orthogonal, though initially noncomputable, projection $\mathscr{S} : C^\infty(\partial\Omega) \to A^\infty(\partial\Omega)$. The projections are related by the equation,

$$\mathscr{S}(\mathscr{I} + \mathscr{A}) = \mathscr{C}, \tag{1}$$

where $\mathscr{I}$ is the identity operator and $\mathscr{A} = \mathscr{C} - \mathscr{C}^*$ is the Kerzman–Stein operator. In the next section we will see how this leads to a simple way for computing the Riemann map and Ahlfors map.

The effectiveness of the Kerzman–Stein equation balances on the fact that the Kerzman–Stein operator is an integral operator with a well behaved kernel

$$A(z, w) = \frac{1}{2\pi i}\left(\frac{T(w)}{w - z} - \frac{\overline{T(z)}}{\overline{w} - \overline{z}}\right)$$

for $w, z \in \partial\Omega$. Here, $T(w)$ is the unit tangent vector at $w \in \partial\Omega$, so $dw = T(w)\,ds_w$. In particular, the singularities at $w = z$ cancel each other and the kernel is infinitely differentiable on $\partial\Omega \times \partial\Omega$. The significance of this fact is that the Kerzman–Stein operator for a region with finite boundary is compact; that is, it can be approximated in norm by finite rank operators. For details on this point, we direct the reader to any functional analysis text. See, for instance, [Zimmer 1990, Chapter 3].

We leave for the reader to check the claim that the singularities in $A(z, w)$ in fact do cancel. This can be done using a Taylor expansion involving an arc length parametrization of the boundary. (One then makes replacements $w = z(s)$ and $z = z(t)$, so that also $T(w) = z'(s)$ and $T(z) = z'(t)$.) By carrying the expansions a few steps further, one can see additionally that the kernel vanishes precisely when the boundary has constant curvature. It follows that precisely when the region is a disc or half plane, the Cauchy and Szegő projectors are the same.

We also leave for the reader to check the analogue of the Kerzman–Stein equation for the example from linear algebra. In this case, the orthogonal projector is

represented by the matrix

$$\begin{pmatrix} \frac{4}{5} & \frac{2}{5} \\ \frac{2}{5} & \frac{1}{5} \end{pmatrix}$$

and the adjoint operator, needed for the computation of $\mathcal{A} = \mathcal{C} - \mathcal{C}^*$, is gotten by taking the transpose of the matrix.

5. Relationship to the Riemann map and Ahlfors map

As described in the introduction, the Riemann map is the essentially unique conformal map from a simply connected region to the unit disc; the Ahlfors map is the essentially unique such conformal map for a multiply connected region. These maps can be expressed as analytic functions with nonvanishing derivatives. In particular, by manipulating the Cauchy–Riemann equations, one can show that at an arbitrary point $z_0 \in \Omega$, an analytic function f accomplishes a rotation by angle $\arg f'(z_0)$. This rotation is paired with a uniform dilation at z_0 by factor $|f'(z_0)|$.

A fundamental relationship between the Riemann map or Ahlfors map and the Szegő projector can be derived using a transformation law for the Szegő kernel. Indeed, the Szegő projector is an integral operator whose kernel can be represented in terms of an orthonormal basis for $A^\infty(\partial\Omega)$. If $\{\phi_j\}_{j \in \mathbb{N}}$ is such a basis, then

$$S(z, \overline{w}) = \sum_{j \in \mathbb{N}} \phi_j(z)\overline{\phi_j(w)},$$

and for a general function f,

$$\mathcal{S}f(z) = \int_{w \in \partial\Omega} S(z, \overline{w})f(w)\, ds_w.$$

From the work of Kerzman and Stein, it follows that the Szegő kernel is the solution to the integral equation

$$S(z, \overline{z}_0) - \int_{w \in \partial\Omega} A(z, w)\, S(w, \overline{z}_0)\, ds_w = \frac{1}{2\pi i} \frac{\overline{T(z)}}{\overline{z}_0 - \overline{z}} \quad \text{for } z \in \partial\Omega, \; z_0 \in \Omega. \quad (2)$$

This equation can be seen to follow from (1). In particular, by taking adjoints of (1) one obtains $(\mathcal{I} - \mathcal{A})\mathcal{S} = \mathcal{C}^*$, and following this, one utilizes an approximate identity to obtain (2).

As will be needed, for the case of the unit disc, Δ, one can use a basis $\{\phi_j\}_{j \in \mathbb{N}}$ where $\phi_j(z) = z^{j-1}/\sqrt{2\pi}$ in order to see that

$$S(z, \overline{w}) = \frac{1}{2\pi} \sum_{j \in \mathbb{N}} z^{j-1}\overline{w}^{j-1} = \frac{1}{2\pi} \frac{1}{1 - z\overline{w}}.$$

This is consistent with the earlier observation for the disc that the Szegő projector and Cauchy projector are the same. Indeed, the Cauchy projector for the disc has

kernel

$$C(z, w) = \frac{1}{2\pi i} \frac{T(w)}{w - z} = \frac{1}{2\pi i} \frac{i w}{w - z} = \frac{1}{2\pi} \frac{1}{1 - z\overline{w}}.$$

In the remainder of this section we derive the relationship between the Szegő kernel and Riemann map for a simply connected region. The derivation for the Ahlfors map is handled differently, although the implementation will be the same. This is discussed in the next section. In the next section we also provide details for the numerical solution of (2).

Assuming then that $f : \Omega_1 \to \Omega_2$ is bianalytic, that is, analytic with an analytic inverse, one can show that the operator $\Lambda : C^\infty(\partial\Omega_2) \to C^\infty(\partial\Omega_1)$ defined according to $\Lambda\phi = (\phi \circ f) \cdot \sqrt{f'}$ sends an orthonormal basis for $A^\infty(\partial\Omega_2)$ to an orthonormal basis for $A^\infty(\partial\Omega_1)$. It follows that

$$S_1(z, \overline{w}) = S_2(f(z), \overline{f(w)}) \, f'(z)^{1/2} \, \overline{f'(w)^{1/2}}$$

where S_1, S_2 are the Szegő kernels for Ω_1, Ω_2, respectively. Applying this result to the case of the Riemann map $f : \Omega \to \Delta$ normalized for $z_0 \in \Omega$ so that $f(z_0) = 0$ and $f'(z_0) > 0$, one finds that

$$S(z, \overline{z}_0) = \frac{f'(z)^{1/2} f'(z_0)^{1/2}}{2\pi}.$$

From this it follows that

$$f'(z) = \frac{2\pi \, S(z, \overline{z}_0)^2}{S(z_0, \overline{z}_0)}, \tag{3}$$

where the relationship holds first for $z \in \Omega$, and then by continuity, it holds for $z \in \overline{\Omega}$. There is a simple equation for relating the boundary values of f to those of f'. So provided with an efficient algorithm for computing the Szegő kernel, we will have an efficient method for computing the Riemann map.

6. Numerical implementation

We now begin with a region Ω that can be described as the interior of n finite curves that are parametrized by smooth functions $z = z_j(t)$ defined for $0 \leq t \leq \ell_j$ such that $z_j(\ell_j) = z_j(0)$ and $z_j'(t)$ is nonvanishing, $1 \leq j \leq n$. Of course, if the region is simply connected, then $n = 1$ and one can drop the subscripts. It is not necessary that the parametrizations be given according to arc length, but it is necessary that the curves are oriented positively with respect to Ω. We further specify a point $z_0 \in \Omega$ that we anticipate having mapped to the origin without rotation.

We first adapt the method used in [Kerzman and Trummer 1986] to compute the
Szegő kernel. In particular, after making the replacements

$$\phi_j(t) = |z'_j(t)|^{1/2} (2\pi i)^{-1} (z'_j(t)/|z'_j(t)|) (\overline{z}_0 - \overline{z}_j(t))^{-1},$$

$$a_{j,k}(t, s) = |z'_j(t)|^{1/2} |z'_k(s)|^{1/2} A(z_j(t), z_k(s)),$$

$$\psi_j(t) = |z'_j(t)|^{1/2} S(z_j(t), \overline{z}_0),$$

Equation (2) becomes

$$\psi_j(t) - \sum_{k=1}^{n} \int_0^{\ell_k} a_{j,k}(t, s)\psi_k(s) \, ds = \phi_j(t) \tag{4}$$

for $0 \leq t \leq \ell_j$ and $1 \leq j \leq n$. With parametrizations provided, the functions ϕ_j and
$a_{j,k}$ are explicitly computable. We wish to solve these equations for the functions
$\psi_j(t)$ in order to have the Szegő kernel.

Perhaps the easiest way to solve (4) is via the Nyström method. For $m > 0$ one
partitions the intervals $[0, \ell_j]$ using $0 = s_0^j < s_1^j < s_2^j < \cdots < s_m^j = \ell_j$ and replaces
(4) by its approximation

$$\psi_j(t) - \sum_{k=1}^{n} \sum_{l=1}^{m} a_{j,k}(t, s_l^k)\psi_k(s_l^k) \, \Delta s_l^k = \phi_j(t). \tag{5}$$

Here, $\Delta s_l^k \overset{\text{def}}{=} s_l^k - s_{l-1}^k = \ell_k/m$. This equation is next solved explicitly for $\psi_j(t)$
when $t = s_i^j$. Indeed, after replacing $t = s_i^j$, this is tantamount to solving a system
of nm linear equations in nm complex unknowns,

$$(I - B)x = y,$$

where the skew-hermitian matrix B has entry $a_{j,k}(s_i^j, s_l^k)$ in its $(n(j-1)+i)$-th
row and $(n(k-1)+l)$-th column. With this setup, the $(n(k-1)+l)$-th entry in
column vector x is $\psi_k(s_l^k)$ and the $(n(j-1)+i)$-th entry in column vector y is
$\phi_j(s_i^j)$.

With values for $\psi_j(s_i^j)$ now determined, the general values for $\psi_j(t)$ can be
recovered from (5). In particular, we set

$$\psi_j(t) = \phi_j(t) + \sum_{k=1}^{n} \sum_{l=1}^{m} a_{j,k}(t, s_l^k)\psi_k(s_l^k) \, \Delta s_l^k, \tag{6}$$

where on the right side we use the values $\psi_k(s_l^k)$ already determined. It may appear
that with this formula we are redefining $\psi_j(t)$ for $t = s_i^j$, when in fact we are not,
since (6) is identical with (5).

Alternatively, we have found it to be effective to replace this last step with a sim-
ple linear interpolation of the values $\psi_j(s_i^j)$ for $1 \leq i \leq m$. In our implementation
this helps to prevent the repeated evaluations of ϕ_j and $a_{j,k}$ that otherwise would
be needed. (The evaluations may have complicated expressions embedded in the

parametrizations.) To be sure, `Riemann_Map()` seems most effective without the additional evaluations—with linear interpolation one can rather increase m for a finer partition, and as a result, obtain better image resolution.

With values of the Szegő kernel $S(z, \overline{z}_0)$ now known for a designated $z_0 \in \Omega$ and for $z \in \partial\Omega$, we look to recover values for the Riemann map and Ahlfors map. We introduce boundary correspondence functions $\theta_j = \theta_j(t)$ defined for $0 \leq t \leq \ell_j$ by

$$f(z_j(t)) = e^{i\theta_j(t)},$$

where $f : \Omega \to \Delta$ is the Riemann map or Ahlfors map. Of course, the θ_j are real and unique only to a multiple of 2π. Differentiating this equation gives

$$f'(z_j(t)) \, z_j'(t) = i\theta_j'(t) \, e^{i\theta_j(t)} = i\theta_j'(t) \, f(z_j(t)),$$

so that in the simply connected case, we obtain from (3) that

$$
\begin{aligned}
f(z_j(t)) &= \frac{f'(z_j(t))z_j'(t)}{i\theta_j'(t)} = \frac{z_j'(t)}{i\theta_j'(t)} \frac{2\pi \, S(z_j(t), \overline{z}_0)^2}{S(z_0, \overline{z}_0)} \\
&= \frac{2\pi}{i\theta_j'(t)} \frac{z_j'(t)}{|z_j'(t)|} \frac{\psi_j(t)^2}{S(z_0, \overline{z}_0)}.
\end{aligned}
\tag{7}
$$

Many factors in this equation are positive, so taking arguments yields simply

$$\theta_j(t) = \arg(-i z_j'(t)\psi_j(t)^2). \tag{8}$$

With the boundary values of the Riemann map now determined, one can obtain the interior values via the Cauchy integral formula, where the integrals can be evaluated using the same Riemann sum approximations used earlier in this section.

We mention that there is another way to recover the boundary correspondence function that is better suited for regions with corners. In particular, by taking the modulus of both sides of (7), we obtain

$$\theta_j'(t) = \frac{2\pi \, |\psi_j(t)|^2}{S(z_0, \overline{z}_0)}, \quad \text{where } S(z_0, \overline{z}_0) = \sum_{k=1}^{n} \int_0^{\ell_k} |\psi_k(t)|^2 dt. \tag{9}$$

The correspondence functions can be obtained via integration, using initial conditions derived using (8). This method results in correspondence functions that are continuous at the corners, as they should be, avoiding errors caused by taking the argument of the tangent vector.

It takes us outside the scope of our discussion to establish these formulas for multiply connected regions, but we mention that (8) remains valid for $n > 1$. This follows from an argument based on the identity relating the Szegő and Garabedian kernels [Bell 1992, page 24]. It is not clear to us if (9) remains valid for $n > 1$.

7. The Sage package `Riemann_Map()`

Led by examples, we now give a brief description of the package, `Riemann_Map()`, which was constructed using the methods of the previous sections. We encourage those who are new to Sage to try the examples online by first setting up a free account at http://www.sagemath.org. (We have published there a worksheet 'Riemann_Map() illustrated' that contains the examples.) For each case, we show both the text to be entered in a cell of a worksheet and the Sage output that follows the cell's evaluation. As typical in Sage, one can find documentation for the package by evaluating a cell that contains only the question `Riemann_Map?`.

Example 1: The Riemann map for an ellipse. To use `Riemann_Map()` for a parametrized ellipse (Figure 4), one provides three variables: a function parametrizing the boundary of the ellipse and whose domain is the interval $[0, 2\pi]$, the derivative of this function, and a complex number identifying the point inside the ellipse that is to be mapped to the origin without rotation. To generate a representation for the Riemann map, one subsequently applies the methods `plot_colored()` and `plot_spiderweb()` in order to have a combined representation showing the coloring of the region and the contour overlay. One obtains sharper resolution by increasing the value of `plot_points` at the expense of increased processing time.

```
z(t) = exp(I*t) +.5*exp(-I*t)   # Riemann map for an ellipse
zp(t) = I*exp(I*t) -.5*I*exp(-I*t)
m = Riemann_Map([z],[zp],0)
p = m.plot_colored(plot_points=500) +m.plot_spiderweb()
show(p,axes=false)
```
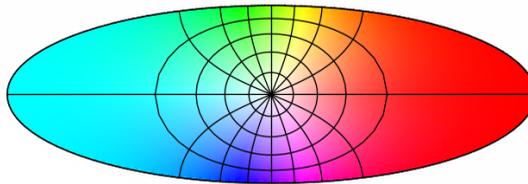

Figure 4. Color representation of the Riemann map for an ellipse.

Example 2: The Riemann map for a square. For a square (Figure 5), one can proceed as for the ellipse using piecewise-defined functions for the parametrization and its derivatives. Alternatively, one can utilize the `polygon_spline()` package along with its methods `value()` and `derivative()` to get these functions more quickly. It is worth noting that command syntax in Sage is shared with the programming language Python, so there is carry-over to learning either of the two languages. We also mention that in the contour overlay, we have increased the

```
ps = polygon_spline([(-1,-1),(1,-1),(1,1),(-1,1)])
z = lambda t: ps.value(t)            # Riemann map for a square
zp = lambda t: ps.derivative(t)
m = Riemann_Map([z],[zp],.3+.3*I)
p = m.plot_colored(plot_points=1000) +m.plot_spiderweb(pts=150)
show(p,axes=false)
```
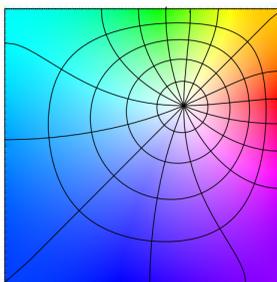

Figure 5. Color representation of the Riemann map for a square.

number of points used to draw concentric rings and radial lines from the default 32 to 150. The extra precision was needed so that the radial lines appear perpendicular to the boundary as they should be.

Example 3: The Ahlfors map for an annulus. For an annulus (Figure 6), one proceeds as in the case of an ellipse, using a parametrization for each of the boundary components. We mention that when `Riemann_Map()` is called, it is necessary that

```
z1(t) = 2*exp(I*t)               # Ahlfors map for an annulus
z1p(t) = 2*I*exp(I*t)
z2(t) = exp(-I*t); z2p(t) = -I*exp(-I*t)
m = Riemann_Map([z1,z2],[z1p,z2p],sqrt(2)*I)
p = m.plot_colored(plot_points=1000) +m.plot_boundaries()
show(p,axes=false)
```
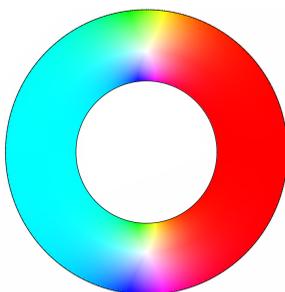

Figure 6. Color representation of the Ahlfors map for an annulus.

the outside curve is provided first in each list of functions. One also must be careful to give parametrizations that are oriented positively with respect to the interior region. Finally, we mention that the methods are not yet sufficiently developed to provide contour overlays for regions with more than one boundary component.

Example 4: The Ahlfors map for a triply connected region. As one more example that combines the elements of the previous examples, we draw the Ahlfors map for a triply connected region composed of a rectangle with two discs removed; see Figure 7. It should be apparent for this example that the Ahlfors map is 3-to-1. As for the previous example, we overlaid the color plot with the region's boundary — this makes the boundary more pronounced and conceals the nearby graininess.

Example 5: The Riemann map for a general region. For our final example, illustrated in Figure 8, we use the companion package `complex_cubic_spline()` to show how to map regions whose boundary is provided by a set of points to be interpolated. For this example, we generated three lists of points which sample two line segments and a circular arc. The combined list of 600 points is suggestive of the boundary of a region that is well-approximated by splines. The subsequent methods `value()` and `derivative()` provide functions giving a parametrization and its derivative for a cubic spline interpolant of the given list. It is worth noting that it is not necessary for the points in the list to be equally spaced, just as it is not necessary for parametrizations to have constant speed.

```
ps = polygon_spline([(-4,-2),(4,-2),(4,2),(-4,2)])
z1 = lambda t: ps.value(t); z1p = lambda t: ps.derivative(t)
z2(t) = -2+exp(-I*t); z2p(t) = -I*exp(-I*t)
z3(t) = 2+exp(-I*t); z3p(t) = -I*exp(-I*t)
m = Riemann_Map([z1,z2,z3],[z1p,z2p,z3p],0)
p = m.plot_colored(plot_points=1000) +m.plot_boundaries()
show(p,axes=false)
```
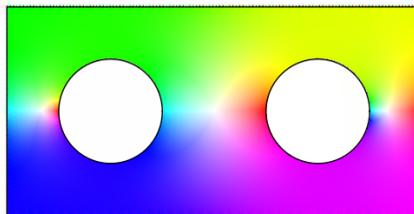

Figure 7. Representation of the Ahlfors map for a triply connected region.

```
li1 = [(sqrt(3)-I)*(t/200)-(3+I)*(1-t/200) for t in range(200)]
li2 = [2*exp(pi*I*(t-100)/600) for t in range(200)]
li3 = [(sqrt(3)+I)*(1-t/200)-(3+I)*(t/200) for t in range(200)]
cs = complex_cubic_spline(li1+li2+li3)
m = Riemann_Map([lambda x: cs.value(x)], \
                    [lambda x: cs.derivative(x)],1-.25*I)
p = m.plot_colored(plot_points=1000) +m.plot_spiderweb(pts=64)
show(p,axes=false)
```
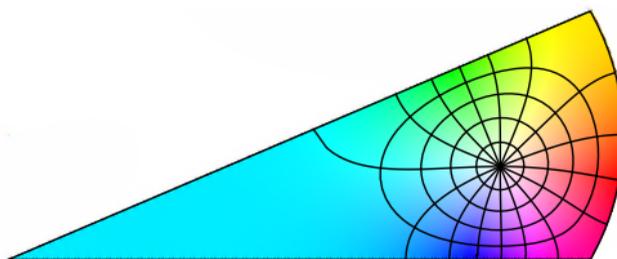

Figure 8. Color representation of the Riemann map for a general region.

References

[Bell 1992] S. R. Bell, *The Cauchy transform, potential theory, and conformal mapping*, CRC Press, Boca Raton, FL, 1992. MR 94k:30013

[Boas 2010] R. P. Boas, *Invitation to complex analysis*, 2nd ed., Mathematical Association of America, Washington, DC, 2010. MR 2674618 Zbl 05769949

[D'Angelo 2010] J. P. D'Angelo, *An Introduction to Complex Analysis and Geometry*, American Mathematical Society, 2010.

[Farris 1998] F. A. Farris, "Reviews: Visual Complex Analysis", *Amer. Math. Monthly* **105**:6 (1998), 570–576. MR 1543280

[Garabedian 1991] P. R. Garabedian, "A simple proof of a simple version of the Riemann mapping theorem by simple functional analysis", *Amer. Math. Monthly* **98**:9 (1991), 824–826. MR 92j:30009 Zbl 0741.30007

[Kerzman and Stein 1978] N. Kerzman and E. M. Stein, "The Cauchy kernel, the Szegö kernel, and the Riemann mapping function", *Math. Ann.* **236**:1 (1978), 85–93. MR 58 #6199

[Kerzman and Trummer 1986] N. Kerzman and M. R. Trummer, "Numerical conformal mapping via the Szegő kernel", *J. Comput. Appl. Math.* **14**:1-2 (1986), 111–123. MR 87f:30017

[Murid et al. 1998] A. H. M. Murid, M. Z. Nashed, and M. R. M. Razali, "Numerical conformal mapping for exterior regions via the Kerzman–Stein kernel", *J. Integral Equations Appl.* **10**:4 (1998), 517–532. MR 99k:30008 Zbl 0919.30008

[O'Donnell and Rokhlin 1989] S. T. O'Donnell and V. Rokhlin, "A fast algorithm for the numerical evaluation of conformal mappings", *SIAM J. Sci. Statist. Comput.* **10**:3 (1989), 475–487. MR 90h:65034 Zbl 0672.30006

[Thomas 1996] A. D. Thomas, "Conformal mapping of nonsmooth domains via the Kerzman–Stein integral equation", *J. Math. Anal. Appl.* **200**:1 (1996), 162–181. MR 97h:46038 Zbl 0846.30005

[Trummer 1986] M. R. Trummer, "An efficient implementation of a conformal mapping method based on the Szegő kernel", *SIAM J. Numer. Anal.* **23**:4 (1986), 853–872. MR 87k:30013

[Zimmer 1990] R. J. Zimmer, *Essential results of functional analysis*, University of Chicago Press, Chicago, IL, 1990. MR 91h:46002 Zbl 0708.46001

mbolt@calvin.edu   *Department of Mathematics and Statistics, Calvin College, 3201 Burton St., S.E., Grand Rapids, MI 49546, United States* http://www.calvin.edu/~mdb7/

sarah.snoeyink@colorado.edu   *Department of Mathematics, University of Colorado at Boulder, Campus Box 395, Boulder, CO 80309, United States*

esv5@students.calvin.edu   *Department of Mathematics and Statistics, Calvin College, 3201 Burton St., S.E., Grand Rapids, MI 49546, United States*

involve

pjm.math.berkeley.edu/involve

involve